Direct Numerical Simulation of Time Evolution of Vortex Ring

Masanori Hashiguchi[1]
[1]Keisoku Engineering System Co., Ltd., 1-9-5 Uchikanda, Chiyoda-ku, Tokyo, 101-0047, Japan

Abstract: Direct numerical simulations (DNS) of the incompressible Navier-Stokes equations are conducted to study time-evolution of a vortex ring in a tube. Flow field is assumed as 2D-axisymmetric. Finite-element analysis is executed by using commercial software, COMSOL Multiphtsics®. It was found that the present computation agrees qualitatively and quantitatively with the existing results of the direct numerical simulations based on finite-difference method which has been reported by Danaila and Helie (2008) .

Keywords: confined vortex ring, 2D axisymmetric flow, DNS, finite-element method.

1. Introduction

There is a growing need for very small, maneuverable, Autonomous Underwater Vehicles (AUV) or underwater drones of long operating duration for surveying deep undersea or the surface of the earth with the aid of acoustic and photographic devices. Efficient fluid system which can be useful for propulsion and maneuver system of UAV, has been desired.

It has been well known that slow moving animals such as jellyfish generate a vortex ring by using contractions of an umbrella-shaped structure for swimming (Kamran Mohseni 2006) instead of jet propulsion. Laboratory experiments have demonstrated that the leading vortex makes a larger contribution to mass and momentum transport than an straight jet of fluid. Therefore, there are practical and scientific interests in the vortex ring generation.

The studies of vortex ring can be traced back more than one and half centuries. A series of theoretical studies have been made for the mathematical description of vortex ring. According to Danaila et al. (2015), we review this briefly as the followings: an early example is the famous Hill's vortex, which assumes that vorticity is linearly proportion to radius within a spherical volume, with potential flow outside. Fraenkel extended the theoretical solution of the vortex filament to account for a small finite thickness. Norbury bridged the models of the Hill's spherical vortex and Fraenkel's thin ring as two asymptotic members of a series of generalized vortex rings, which is referred to as the Norbury –Fraenkel vortex ring family. This family predicts more accurate streamlines and more precise vortex ring outlines. However, its linear distribution of vorticity is still unrealistic (Danaila and Helie 2008).

Radially confined vortex ring flows have been far less studied compared with unconfined vortex rings, despite their importance for many practical applications. Recently Danaila and Helie (2008) conducted Direct Numerical Simulation (DNS) of the Navier-Stokes equations based on finite-difference method on the investigation of axisymmetric vortex rings evolving in a tube and reported elliptical cross-sections and radial asymmetry for the vorticity distribution, which the Norbury-Fraenkel model is unable to capture. Recent experimental study by Stewart et al. (2012) demonstrated important differences between the evolution of a vortex ring confined in a tube and its evolution in an unbounded domain such as higher decay rates of circulation on vortex rings confined in a tube.

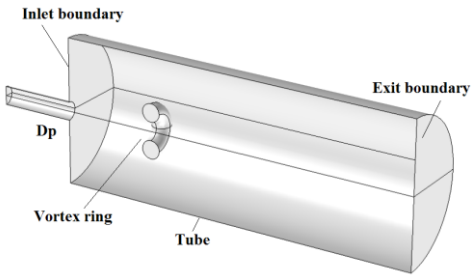

Figure 1. Schematic view of confined vortex ring.

In this paper we conduct a direct numerical simulation based on the Navier-Stokes equations to investigate time evolution of an axisymmetric vortex ring in a tube ejected from the nozzle with time-dependent piston motion. Numerical solutions are obtained based on finite-element analysis, where commercial software, COMSOL Multiphysics ® is used. The solutions obtained here are compared with the results of Danaila and Helie (2008).

2. Method of Approach

2.1 Computational conditions

Figure 1 shows schematic view of the vortex ring in a tube. The nozzle for the ejection of fluid to generate the vortex ring is attached to the bottom end of the tube. The diameter of the nozzle is Dp. The average velocity of the flow ejected from the nozzle is Wp. The Reynolds number, Re, is defined by DpWp/ν , where ν is the kinematic viscosity of the fluid. Figure 2 shows the model dimensions and boundary conditions.

The incompressible Navier-Stokes equations and the continuity equation in Cartesian coordinates are:

$$\frac{\partial \mathbf{u}}{\partial t} + (\mathbf{u}\cdot\nabla)\mathbf{u} = -\frac{1}{\rho}\nabla p + \frac{\mu}{\rho}\nabla^2\mathbf{u}$$

$$\nabla\cdot\mathbf{u} = 0$$

where t is the time, **x** the components of Cartesian coordinate system, ρ the fluid density, p the fluid pressure, μ the viscosity and **u** the fluid velocity vector.

In the present study, the flow is assumed to be 2D-axisymmetric. Thus the flow field is easily described in cylindrical coordinates (r, z).

Numerical modelling the piston-cylinder vortex generator is very important. We modelled the piston-cylinder vortex generator as the inlet flow boundary conditions with the same procedure of Danaila and Helie (2008).

$$V_z(t,r) = V_0(t)V_{zb}(r)$$

$$V_0(t) = \begin{cases} \dfrac{W_p}{2}\left\{1+\tanh\left[\dfrac{5}{\tau_1}(t-\tau_1)\right]\right\}, \\ t \le \tau_1 + \tau_2/2 \\ \dfrac{W_p}{2}\left\{1+\tanh\left[\dfrac{5}{\tau_1}(\tau_1+\tau_2-t)\right]\right\}, \\ t > \tau_1 + \tau_2/2. \end{cases}$$

$$V_{zb}(r) = \frac{1}{2}\left\{1+\tanh\left[\frac{1}{2\delta_w}\left(\frac{D_p}{2r}-\frac{2r}{D_p}\right)\right]\right\}$$

Physical parameters in the present simulation are as followings: the Reynolds number is Re=1400 and the stroke ratios are Lp/Dp=2, 4 and 6. The value of the parameter τ_2 is determined as to be equal to the stroke ratio Lp/Dp. The acceleration/deceleration time of the impulsive piston motion τ_1 is 0.15. The dimensionless thickness of the vorticity layer at the inlet δ_w is 0.05.

All the quantities to be presented will be normalized using the characteristic length Dp, velocity Wp, and time Dp/Wp.

2.2 Direct numerical simulation

Finite-element analysis of the incompressible Navier-Stokes equations is conducted in the present study. Usually, numerical stabilization techniques such as streamline diffusion and crosswind diffusion are necessary for flow computation of viscous flow of high Reynolds numbers. If the space domain of the flow field to be computed is discretized with a sufficient number of mesh and proper spatial arrangement of it, we could get a numerical solution of the Navier-Stokes equations without numerical stabilization techniques. We call this type of simulation as direct numerical simulation (DNS). In the laminar flow interface of COMSOL Multiphysics®, we can easily switch-off the numerical stabilization. Figure 2 shows the mesh system used in this study. The validity of this mesh system will be proven when vortex patterns resulting from the present computation compares with those of Danaila and Helis's (2008).

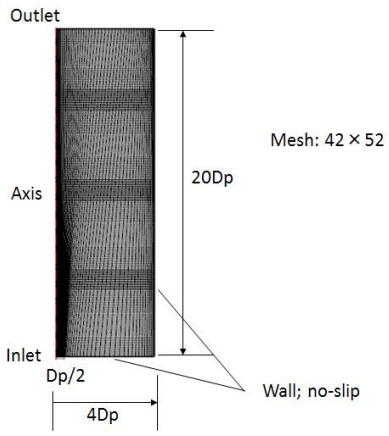

Figure 2. Mesh system.

They used a fractional step method based on the combination of a third-order Runge-Kutta scheme for the convective terms and a semi-implicit Crank-Nicolson scheme for the viscous terms, which is globally second order accurate in space and time.

On the other hand, there is the Ladyzenskaya-Babuska-Brezzi condition (LBB condition) for viscous flow computation due to finite-element analysis. Therefore we used P2-element for the flow velocity field and P1-element for the pressure field. We also can easily select these shape functions in the COMSOL setup.

3. Results and discussions

First we examined a typical evolution of the vortex ring for the case of Lp/Dp =6. Figure 3 shows the computed azimuthal vorticity components normalized by the maximum values. The contour lines (min=0.05, max=0.95, increment=0.05) were plotted at t=10, 15.4 and 20. These results agree with Danaila and Helie (2008 Fig,2). A clear pinch-off of the vortex ring is also observed in our simulation at t=15.4, where the contour line of 0.05 encircles the vortex.

Secondly we examined the evolution of the azimuthal vorticity fields for different stroke ratio Lp/Dp =2, 4 and 6. Figures 4 and 5 show our results. These also agree with those of Danaila and Helie (2008 Fig. 3). For detail examination, we plot velocity profiles through center of the vortex for Lp/Dp =4 and at t=30. Figure 6 shows the agreement quantitatively with the result of Danaila and Helie (2008 Fig.4).

Therefore we can conclude that these comparisons validate the present method.

As reported by Stewart et al. (2008), it is known that when the outer wall approaches vortex ring, the time advancing of vortex wing is retarded due to the wall effect. We examined the wall effect for L_p/D_p=4 as shown in Figures 5 and 6. The radius of the wall of the tube was set to $R_{max}=2D_p$. These results shows the retardation of the time marching of the vortex ring due to the wall effect of the tube.

4. Concluding remarks

We conducted a direct numerical simulation based on the laminar flow interface of COMSOL Multiphysics Ver.5.2a to examine the time evolution of the vortex ring in a tube. As described here, it was found that the results obtained by the present method agree well with the existing literatures related to confined vortex ring. This suggests that the present method become a useful tools to explore new idea in this filed.

5. References

1. Ionut Danaila, Felix Kaplanski, end Sergei Sazhin, Modellinf of confined vortex rings, J. Fluid Mechanics, 774, 267-297(2015).
2. Kamran Mohseni, A formulation for calculating the translational velocity of a vortex ring or pair, BIOINSPIRATION & BIOMIMETICS, 1, S57-S64(2006).
3. Ionut Danaila and Jerome Helie, Numerical simulation of the postformation evolution of a laminar vortex ring, PHYSICS OF FLUIDS, 20, 073602(2008).
4. K.C. Stewart, C.L. Niebel, S. Jung and P.P. Vlachos, The decay of confined vortex rings, Experiments in Fluids, 53, 163-171 (2012).

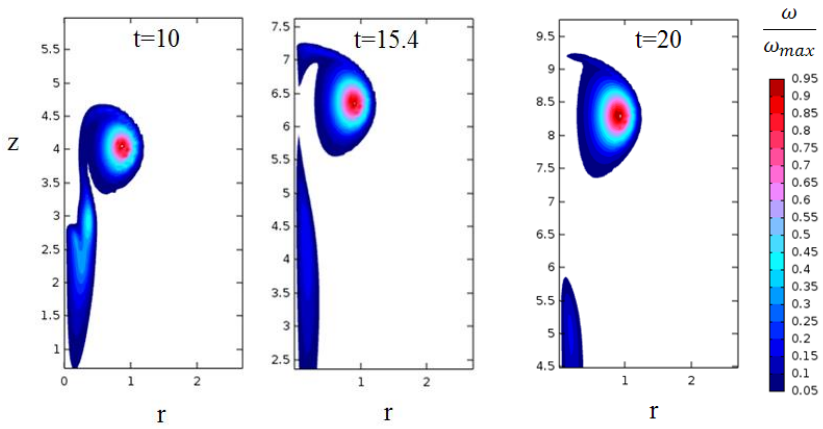

Figure 3. Snapshots of the vorticity fields for Lp/Dp =6 at time t=10, 15.4 and 20.

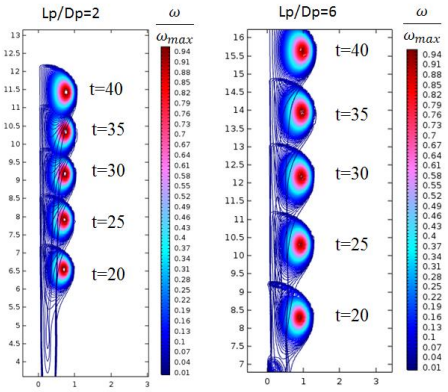

Figure 4. Time evolutions of the vorticity fields for Lp/Dp =2 and 6 at t=20,25,30,35 and 40.

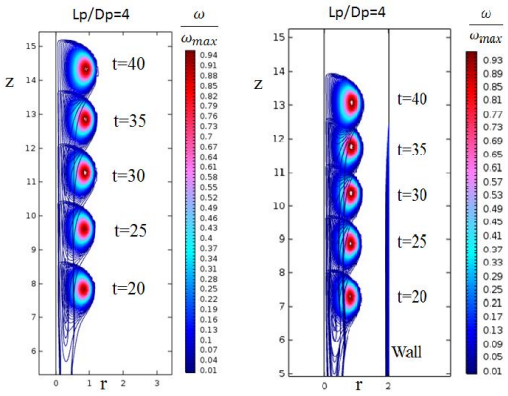

Figure 5. Time evolutions of the vorticity fields for Lp/Dp =4 and the wall effect (right).

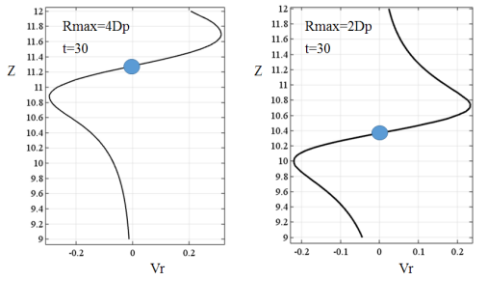

Figure 6. Radial velocity distribution along the line through the center (circle) of vortex ring for Lp/Dp =4 and the wall effect (right).